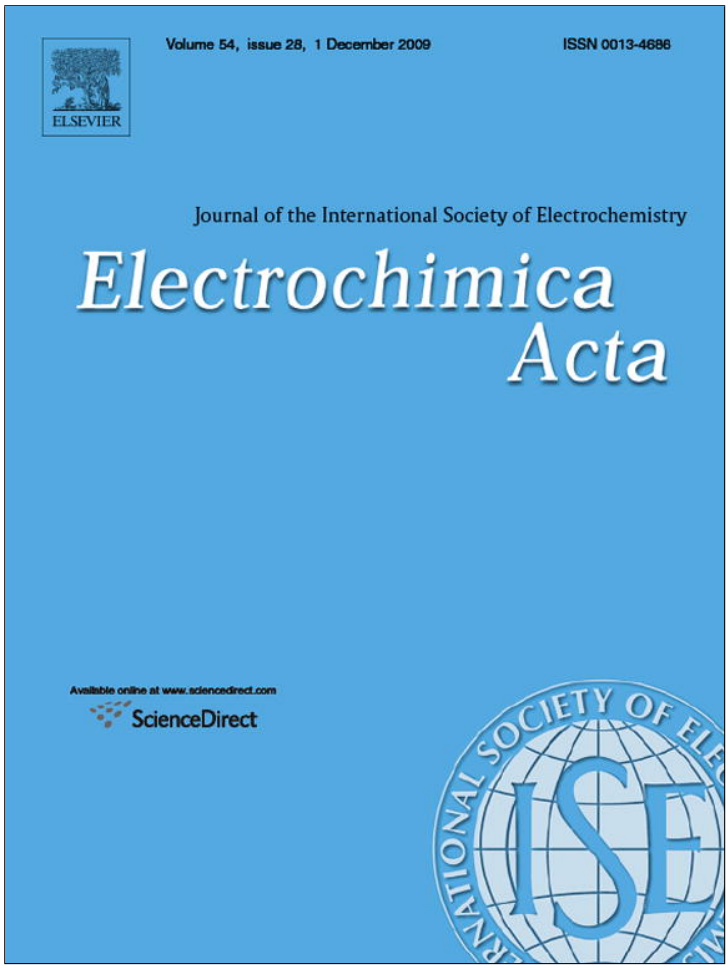

Electrochimica Acta 54 (2009) 7324–7329

Contents lists available at ScienceDirect

Electrochimica Acta

journal homepage: www.elsevier.com/locate/electacta

Copper and brass aged at open circuit potential in slightly alkaline solutions

R. Procaccini, M. Vázquez, S. Ceré *

División Corrosión, INTEMA, Facultad de Ingeniería, Universidad Nacional de Mar del Plata (UNMdP), Juan B. Justo 4302, B7608FDQ Mar del Plata, Argentina

ARTICLE INFO

Article history:
Received 6 April 2009
Received in revised form 15 July 2009
Accepted 18 July 2009
Available online 28 July 2009

Keywords:
Surface films
Oxygen reduction
Copper alloys

ABSTRACT

Surface oxide films were grown on 99.99% copper and brass (copper–zinc alloy, Cu77Zn21Al2) in 0.1 mol L^{-1} borax solution at open circuit potential and were characterized using various experimental techniques. The composition of the passive films formed in situ on the different materials was studied using differential reflectance spectroscopy. The thickness of the oxide layers on copper and brass was compared by chronopotentiometric curves and potentiodynamic reductions. The electrical properties of each oxide were analyzed by means of electrochemical impedance spectroscopy. Their influence on the oxygen reduction reaction was also investigated using voltammetry hydrodynamic tools such as the rotating disk electrode. The results show that the incorporation of Zn to Cu in brass changes the composition and the thickness of the surface film. The films grown on brass tend to be thicker but less resistive and Zn compounds incorporate to the film. This is supported by results from reflectance and impedance spectroscopy. The kinetics of oxygen reduction is strongly inhibited on oxidized electrodes, particularly in the case of brass. The global number of exchanged electrons remains close to four and seems to be independent of the presence of surface oxides.

1. Introduction

The oxygen reduction reaction (ORR) is the main cathodic half reaction of corrosion processes in aerated media. Although the reaction mechanism strongly depends on the surface where it occurs, it has been investigated in a few corrodible metals [1–4].

Copper and its alloys are widely used in numerous applications in civil engineering, power generation and heat exchangers devices among others. It has been demonstrated for copper and copper–nickel alloys, that the oxygen reduction reaction is within the potential region where the metal oxidation produces a $Cu/CuO/Cu_2O$ duplex layer. The reaction proceeds through a chemical electrochemical mechanism where the redox couple Cu_2O/CuO plays a key role in the reduction sequence [5,6]. However, in the case of brass, the presence of Zn cannot be disregarded. The passive film formed on Cu–10Zn and Cu–20Zn is similar to that on copper, where Cu_2O/CuO are the main constituent oxides and the presence of ZnO is confirmed by XPS [7].

Recently, the oxygen reduction reaction has been studied on negatively polarized brass, where the presence of oxides on the surface is kept to a minimum [8]. There, the influence of contaminants, particularly chloride ions has also been investigated. Instead, this work is focused on the study of the passive films formed on copper and brass in situ in 0.1 mol L^{-1} borax solution held 24 h at open circuit potential and the relationship between the oxidized surface and the oxygen reduction reaction.

2. Experimental

Borax 0.1 mol L^{-1} (pH = 9.2) was used as electrolyte. The solutions were deaerated for 15 min with high-purity N_2 prior to each measurement or saturated with O_2 during 15 min, as conveniently indicated. This was enough to guarantee an average oxygen content lower than 1.5×10^{-5} mol L^{-1}. The oxygen concentration in oxygen saturated electrolytes was taken as 1.15×10^{-3} mol L^{-1} in borax solutions. That concentration was measured using a PST3 oxygen meter attached to an optical fiber sensor. All the experiments were carried out at room temperature (20 ± 2 °C).

The electrodes were constructed from spectroscopic grade copper (99.99%) and from aluminium–brass rods (77% Cu, 21% Zn, 2% Al; UNS 68700) provided by LCL Pty Ltd.™, Australia. To carry out optical experiments, metal disks were embedded in epoxy resin and conveniently mounted on PVC holders. A cable for electrical contact was welded at the back side of the disk. When performing electrochemical tests, rotating disk electrodes were prepared from rods of Cu and brass, which were embedded in epoxy resin and mounted in Grilon™ cylindrical holders. Prior to use, the electrodes were abraded with a sequence of emery papers and finally mirror polished with 0.5 μm alumina powder.

The electrochemical measurements were conducted using a standard three-electrode cell. A Pt wire of large-enough area was used as auxiliary electrode. Two different electrodes were used as

* Corresponding author. Tel.: +54 223 481 6600; fax: +54 223 481 0046.
E-mail address: smcere@fi.mdp.edu.ar (S. Ceré).

0013-4686/$ – see front matter © 2009 Elsevier Ltd. All rights reserved.
doi:10.1016/j.electacta.2009.07.058

reference: $Hg/Hg_2SO_4/K_2SO_4$ 0.6 mol L^{-1} (MSE, 0.616 V vs. NHE) for the electrochemical experiments and Ag/AgCl/NaCl 3 mol L^{-1} (0.208 V vs. NHE) when recording reflectance spectra. However, all the potential values will be indicated taking MSE as reference. A Voltalab PGP 201 potentiostat was employed to control current and potential.

To record cyclic voltammograms, the electrolyte was deaerated for 15 min with high-purity N_2 prior to each measurement. The electrodes were then pretreated by holding them at −1.6 V for 10 min to have a reproducible initial condition.

To evaluate the influence of an oxide film on the surface, the electrodes were aged at open circuit potential (OCP) for 24 h.

The composition of the surface films was evaluated using reflectance spectroscopy. The absorption spectra were recorded in situ. Baseline corrections were carried out by polarizing two identical polished surfaces at −1.6 V to prevent oxide growth. The spectrum of each surface was recorded after 24 h at OCP in oxygen saturated electrolyte. The spectroelectrochemical measurements were carried out using a commercial double-beam spectrophotometer (Shimadzu UV 160A), conveniently modified as described elsewhere [9].

To carry out the potentiodynamic reductions of the surface films, the film was reduced in deaerated electrolyte by scanning the potential from OCP to −1.6 V at 0.02 V s^{-1}. The curves were recorded with the electrodes rotating at 400 rpm.

The films were also reduced chronopotentiometrically in deaerated electrolyte by applying a set of constant current densities of −0.25, −0.50 and −1.0 mA cm^{-2} for few minutes until potential changes indicated complete reduction.

Electrochemical impedance spectroscopy (EIS) tests were also performed on electrodes in an oxygen saturated solution. The AC voltage signal amplitude was ±0.005 Vrms and the frequency was varied between 100 kHz and 1 mHz. The results were analyzed using equivalent circuits. The experimental data were fitted to the equivalent circuit using ZView [10]. The circuit chosen to fit the results on aged electrodes (Fig. 1) is used to represent oxide-coated metals. Similar circuit has been used before by other authors [11]. Corroding electrodes can show various types of inhomogeneities, which can be represented by the inclusion of constant phase elements (CPEs) in place of capacitors in the equivalent circuit. Surface roughness, insufficient polishing, grain boundaries and surface impurities have been mentioned among the main reasons allowing the use of CPEs in equivalent circuits of corroding electrodes [12,13]. The impedance of CPEs can be written as:

$$Z_{CPE} = [Q(j\omega)^n]^{-1} \quad (1)$$

where Q is the frequency-independent constant or pseudo-capacitance and n a constant power, with $-1 < n < 1$. A rough or porous surface can cause a double layer capacitance to appear as a constant phase element with n between 0.5 and 1.

The circuit in Fig. 1 presents a Warburg element that could be attributed to a diffusion process taking place in the solid phase. Warburg impedances and CPEs with a n value around 0.5 (the last known as "infinite diffusion") are used to model increasing ionic conductivity due to corrosion processes occurring inside the pores and the consequent diffusion process along them. If the surface layer is thin, low frequencies will penetrate the entire thickness, creating a finite length Warburg element (Eq. (2)):

$$Z_w = \frac{W_R}{(jT\omega)^n}\tanh(jT\omega)^n \quad (2)$$

where W_R is associated with solid phase diffusion and T is related to the effective diffusion coefficient (D) and the effective diffusion thickness (L) by $T = L_2/D$. Only if the material is thick enough so that the lowest frequencies do not penetrate the entire layer, it can be interpreted as infinite diffusion [13].

The oxygen reduction polarization curves were registered at 0.01 V s^{-1}, using at least five different rotation rates between 100 and 1225 rpm. The rotating disk experiments were carried out using a Radiometer™ controller (CTV101). Each rotation rate was recorded as an independent experiment, using an aged electrode, and starting the curve from the OCP and up to the hydrogen evolution region (−1.6 V). Polarization curves on oxide-free surfaces were also recorded for the sake of comparison. In these cases, the electrodes were pretreated by holding them at −1.6 V in the deaerated electrolyte during 15 min. Then, the electrolyte was saturated with oxygen, bubbling the gas for at least 15 min prior to recording the polarization curves. The polarization curves were recorded in the positive direction, starting at −1.6 V.

3. Results and discussion

3.1. Surface characterization by reflectance spectroscopy

Copper and brass were aged at OCP in the borax solution. After the first hour of ageing the open circuit potential attains a stable value: −0.470 ± 0.010 V in the case of copper and −0.480 ± 0.008 V in the case of brass. The reflectance spectra on each surface were recorded after ageing 24 h in oxygen saturated electrolyte and are presented in Fig. 2.

Even when the OCPs of both materials were very similar, noticeable differences were found in their spectra. In the case of copper, the main spectral features of cuprous oxide can be recognized: a shoulder at 560 nm, a broad peak at 360–380 nm, and a lower one at 240 nm [9,14,15]. In the case of brass, the transmittance values are very low between 500 and 800 nm and increase steadily towards the UV region. The spectrum seems to be dominated by the featureless absorption bands of Zn compounds.

The higher absorption of the surface films on brass can be related to the presence of a thicker surface film.

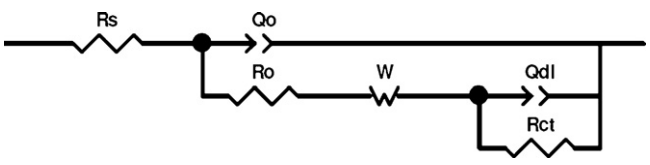

Fig. 1. Equivalent circuit chosen to fit EIS data.

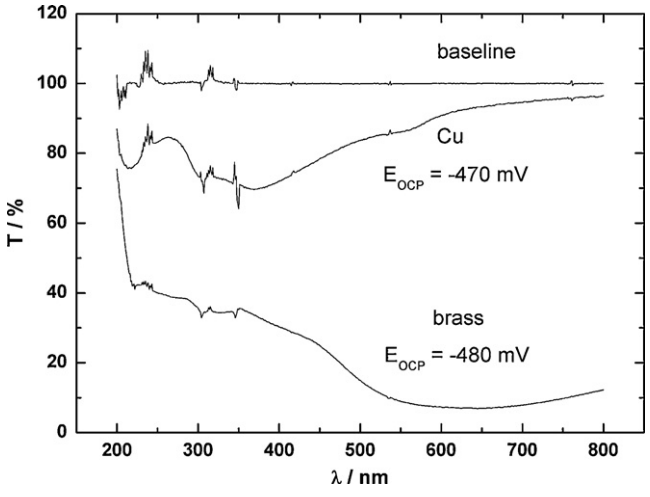

Fig. 2. Differential reflectance spectra for copper and brass in oxygen saturated 0.1 mol L^{-1} borax solution at OCP for 24 h.

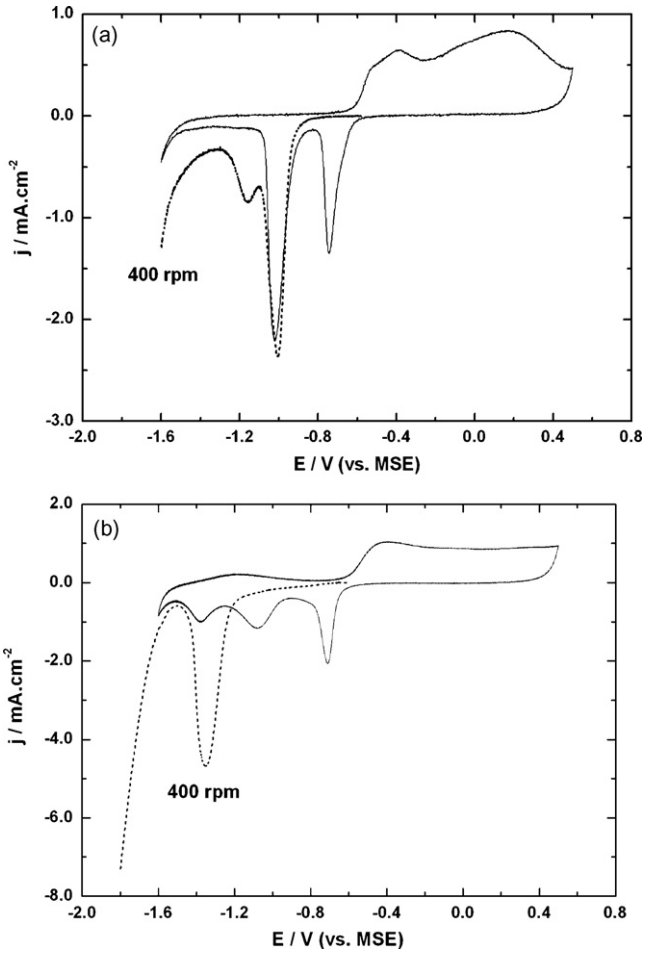

Fig. 3. (a) Voltammogram of copper electrode in contact with deaerated 0.1 mol L^{-1} borax, superimposed to potentiodynamic reduction curve (dashed line) of aged copper electrode at OCP for 24 hs ($\nu = 0.01$ V s^{-1}). (b) Voltammogram of brass electrode in contact with deaerated 0.1 mol L^{-1} borax, superimposed to potentiodynamic reduction curve (dashed line) of aged brass electrode at OCP for 24 h ($\nu = 0.01$ V s^{-1}).

3.2. Surface characterization based on electrochemical techniques

The surface oxohydroxides formed on copper and brass aged during 24 h in borax solution were also reduced by means of potentiodynamic scans and chronopotentiometric curves. The results are presented in Figs. 3 and 4 respectively.

Fig. 3a and b presents the cyclic voltammograms (CVs) for copper and brass respectively, superimposed to the results from the potentiodynamic reduction curves, all of them registered in deaerated borax solution. In the CV of copper, two broad anodic peaks appear at −0.4 V (Cu_2O formation) and at 0.15 V (CuO formation), while the two cathodic peaks are located at −0.75 V (CuO reduction to Cu_2O) and −1.0 V (Cu_2O reduction). The cyclic voltammogram of brass, recorded in the same conditions as those shown for copper, shows a broad anodic peak at −1.2 V (most likely due to a Zn containing specie, as deduced by comparison with the voltammogram of pure Zn [7]), another one at −0.4 V (Cu_2O formation), while a plateau starts at −0.2 V (CuO formation). The cathodic peaks can be seen at −0.7 V (CuO reduction to Cu_2O) and −1.1 V (Cu_2O reduction). A third cathodic peak at −1.35 V is probably due to $HCuO_2^-$ reduction [7].

In Fig. 3a and b, and taking into account the different current density scales, more charge can be observed in reducing the oxides grown on brass, when compared to the situation for copper. This, in turn, can be associated to thicker films, in agreement with the reflectance results discussed above. Also, by comparison to the CVs,

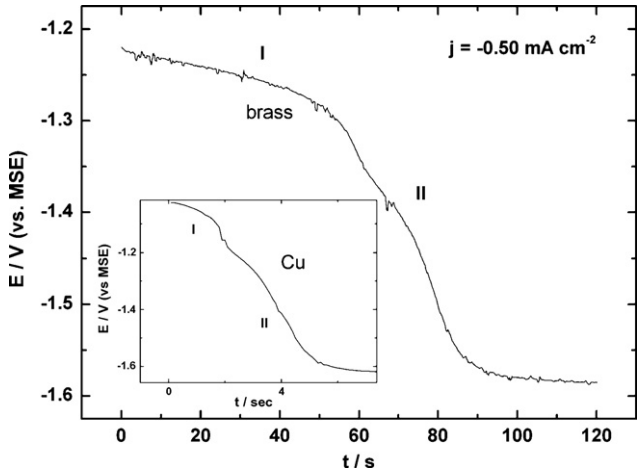

Fig. 4. Chronopotentiometric curves of copper and brass aged for 24 h in deaerated 0.1 mol L^{-1} borax.

it can be observed that the composition of the oxides grown on brass and copper is very different and that the surface film present on brass clearly shows the presence of compounds containing Zn.

The films were also reduced chronopotentiometrically, and the results in Fig. 4 can be used to estimate the charge, since by applying Coulomb's law, the time elapsed up to the potential step is proportional to the charge involved in reducing the film. In agreement with the results in Fig. 3, it can be seen that the charge of the surface film on brass is roughly 20 times bigger than that on copper.

Impedance spectra were also recorded on copper and brass electrodes after 24 h of ageing. The spectra obtained for copper and brass electrodes can be fitted using the equivalent circuit presented in Fig. 1. Many circuits have been proposed to model the behavior of copper in alkaline solution. Recently, Liu et al. [16] presented an interesting study comparing the various equivalent circuits and their respective interpretations, all for copper in contact with chloride containing solutions.

EIS data fit results are shown in Figs. 5 and 6, together with the recorded data. The fitting parameters are presented in Table 1. The experimental data were found to be sufficiently well fitted by the proposed equivalent circuit. Rs represents the solution resistance, Qo the pseudo-capacitance of the surface film, Ro the resistance to current flow through defects in the surface film, Qdl the metal

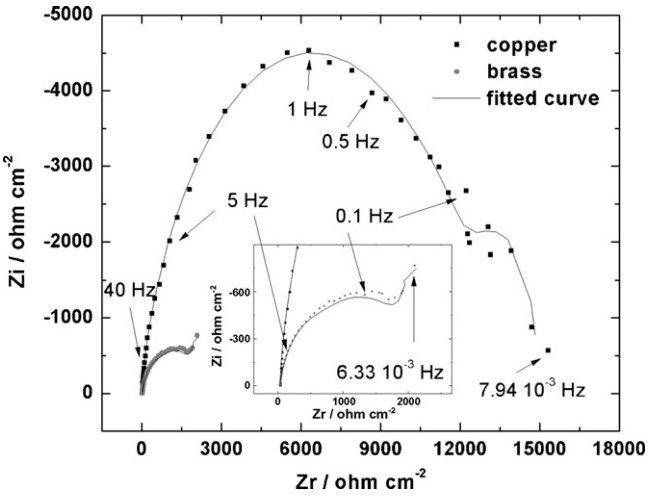

Fig. 5. Impedance spectra (Nyquist plot) recorded on copper and brass electrodes aged at OCP for 24 h in oxygen saturated 0.1 mol L^{-1} borax solution. Data are represented by symbols and fitting results by lines.

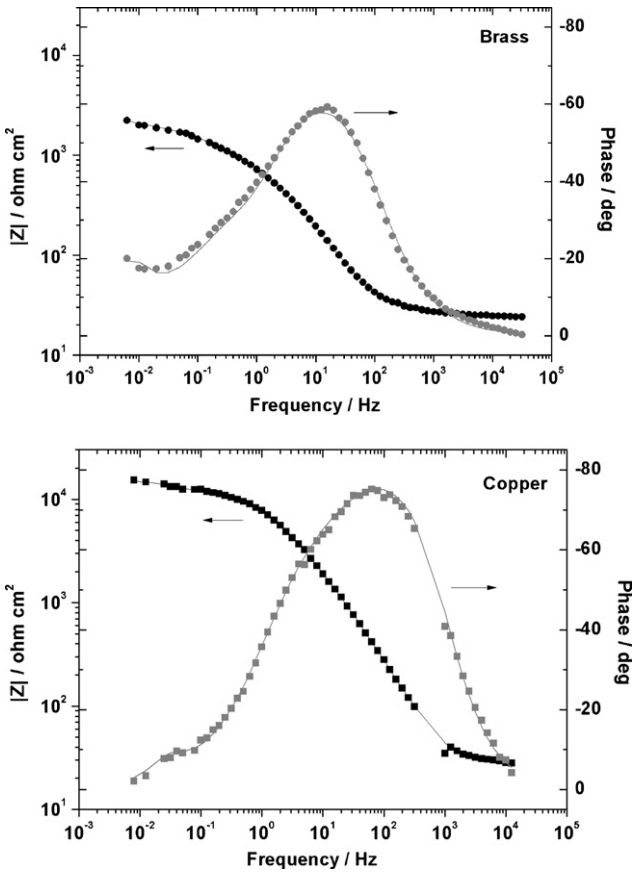

Fig. 6. Impedance spectra (Bode plots) recorded on copper and brass electrodes aged at OCP for 24 h in oxygen saturated 0.1 mol L^{-1} borax solution. Data are represented by symbols and fitting results by lines.

pseudo-capacitance (charging current through the double layer capacitor), Rct the charge-transfer resistance, and *W* represents a Warburg element associated to diffusion through the pores in the film. As can be seen in Fig. 6, the phase angle in the low-frequency range decreases, without reaching zero. This suggests the presence of a porous surface film and the appearance of diffusion effects through this layer [17]. The presence of a porous Cu_2O film on

Table 1
Optimized values for the parameters employed in fitting the data in Figs. 5 and 6 to the equivalent circuit proposed.

Electrode	Element	Value
Cu	Rs/Ω cm²	28.55
	Qo/Ω^{-1} cm^{-2} s^n	8.21×10^{-6}
	n	0.946
	Ro/Ω cm²	3370
	W_R/Ω cm²	4377
	T/s	9.364
	W_n	0.429
	Qdl/Ω^{-1} cm^{-2} s^n	2.01×10^{-5}
	n	0.736
	Rct/Ω cm²	7487
Brass	Rs/Ω cm²	25.12
	Qo/Ω^{-1} cm^{-2} s^n	1.68×10^{-4}
	n	0.828
	Ro/Ω cm²	926
	W_R/Ω cm²	1326
	T/s	49.59
	W_n	0.465
	Qdl/Ω^{-1} cm^{-2} s^n	1.28×10^{-3}
	n	0.769
	Ro/Ω cm²	657

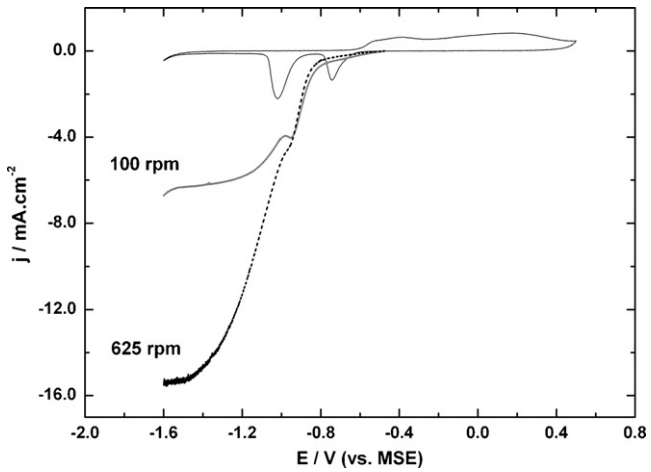

Fig. 7. Set of two RDE polarization curves for copper aged at OCP during 24 h in oxygen saturated 0.1 mol L^{-1} borax solution superimposed to cyclic voltammogram of copper. RDE scan rate: 0.02 V s^{-1}, CV scan rate: 0.01 V s^{-1}.

Cu in sodium tetraborate has been proposed earlier by Abrantes et al. [18]. These authors claim that the growth of the Cu_2O layer may form pores that expose the underlying copper which can then be oxidized directly to Cu(II), in the form of $Cu(OH)_2$. Eventually, growth and dissolution of $Cu(OH)_2$ can then take place via the pores in the underlying layer of Cu_2O.

From the fitting data in Table 1, it can be observed that the pseudo-capacitance of the surface oxide is 100 times higher for brass than for copper. Also, the parameter *T* (see Eq. (2)) associated to the Warburg element, which accounts for the diffusion processes along the pores in the films, is higher for brass. These results can be attributed to a more defective and less dielectric surface film for brass even if it is thicker, in agreement with reflectance results, together with potentiodynamic and chronopotentiometric reductions, as discussed above. Accordingly, W_R is three times higher for Cu than for brass showing that solid phase diffusion is more difficult for Cu than for brass.

Due to the open porous structure of the film, no attempt will be made to calculate oxide thickness from capacitance values. In the present case, the low value of Ro and the high value of Qo for brass are probably indicating that the pores are filled with the electrolyte which make very difficult to estimate permittivity values. The fact that thickness values calculated using impedance results are not in agreement with the ones measured by others techniques has been reported before [7].

3.3. Cathodic polarization curves under hydrodynamic control

Figs. 7 and 8 show typical oxygen reduction *I*–*V* curves registered in oxygen saturated 0.1 mol L^{-1} borax solution on aged copper and brass respectively. These cathodic polarization curves are presented superimposed to the cyclic voltammogram of each material in the same electrolyte (but deaerated), which where discussed in more detail in Section 3.2. On copper, the current increase starts only after CuO has been completely reduced. This reduction is evidenced by a small hump at 0.97 V, as discussed previously. The limiting current develops at potentials negative to this hump, on a predominantly oxide-free surface, and corresponds to a single four-electron process.

To investigate the potential dependence of oxygen reduction, the following equation can be applied [19,20]:

$$E = -\frac{1}{\alpha_c nF}\ln\frac{j}{j_0} + \frac{1}{\alpha_c nF}\ln\left(\frac{j_L}{J} - 1\right) \quad (3)$$

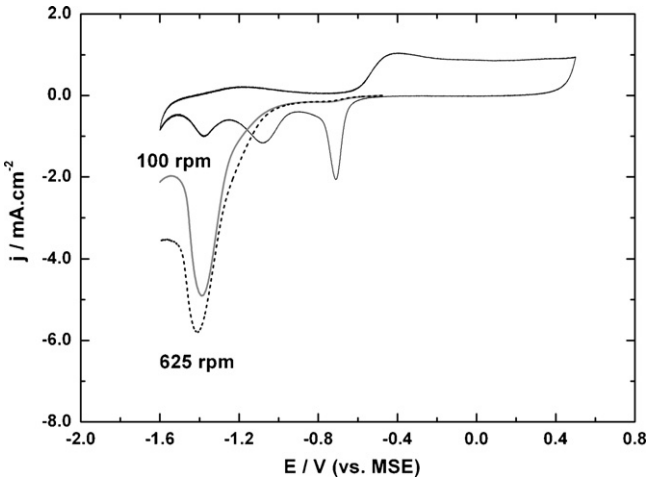

Fig. 8. Set of two RDE polarization curves for brass aged at OCP during 24 h in oxygen saturated 0.1 mol L^{-1} borax solution superimposed to cyclic voltammogram of brass. RDE scan rate: 0.02 V s^{-1}, CV scan rate: 0.01 V s^{-1}.

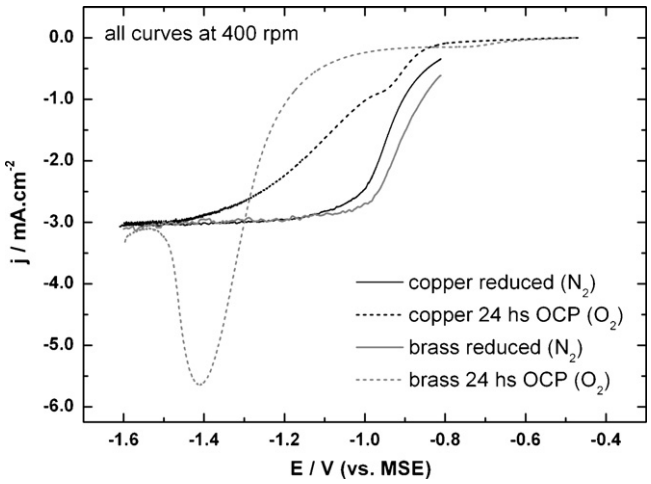

Fig. 10. RDE polarization curves for copper and brass in two different conditions: aged at OCP for 24 h and reduced at −1.6 V.

where j_L is the limit current density, j_0 the kinetic current density, α_c the cathodic transfer coefficient, n the number of exchanged electrons, F the Faraday constant, R the gas constant, T the temperature (Kelvin) and E the applied overpotential.

Fig. 9 shows a test of Eq. (3) for aged copper. The lines show a clear change in the slope at around −1.0 V, in coincidence with the reduction hump observed in the polarization curves. At potentials positive to −1.0 V the plot is difficult to interpret because the observed current corresponds to the reduction of the surface oxides plus the current due to oxygen reduction. However, when the portion of the lines negative to −1.0 V is considered, curves recorded at different rotation rates present a slope of ca. −0.3 V per decade, in agreement with the results obtained for non-oxidized copper surfaces [19]. Even for negatively polarized Cu electrodes, it has been demonstrated that an "oxide-free" surface cannot be obtained. The large values of the Tafel slope would reflect that residual oxides play a key role in the oxygen reduction mechanism. In the case of copper then, the superficial oxides do not have any influence neither on the limit current density, the global number of electrons exchanged nor in the Tafel slopes.

On brass, the oxygen reduction curves are dominated by the reduction of the surface compounds. This reduction peak is located at more negative potentials and presents higher current density

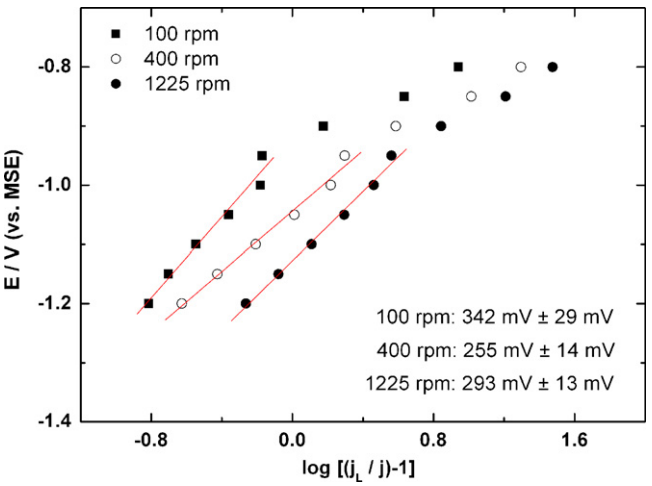

Fig. 9. Tafel plots of aged copper electrodes in contact with 0.1 mol L^{-1} borax solution.

values when compared to the case in copper. These features hinder the classical analysis of the cathodic polarization curves using the Levich equation, since no clear limiting current can be observed until the surface film has been completely reduced. However, the current registered at potentials negative to the peak is still dependent to rotation rate, and if plotted against $\omega^{1/2}$, it follows the Levich equation, rendering a number of exchanged electrons which is close to 4.

The oxygen reduction currents on aged and reduced (oxide-free) electrodes for both materials are compared in Fig. 10. In the potential range where the kinetics is under mix control, both materials show much lower current densities in the aged condition. The fact that copper becomes less active for oxygen reduction as its surface is more oxidized had been reported before [19]. But in this case, the inhibitory effect of an aged surface on the ORR is particularly strong on brass. The presence of corrosion products on the electrode surface has been shown before to inhibit the ORR on corroded Zn [3]. Oxides can slow down the kinetics of the ORR by means of chemical electrochemical (CE) reduction mechanism, such as:

$$Cu_2O + \tfrac{1}{2}O_2 \rightarrow 2CuO \quad \text{(fast)} \tag{1}$$

and/or

$$Zn + \tfrac{1}{2}O_2 \rightarrow ZnO \quad \text{(fast)} \tag{1'}$$

followed by

$$2CuO + 2H_2O + 2e^- \rightarrow Cu_2O + 4OH^- \quad \text{(slow)} \tag{2}$$

and/or

$$ZnO + H_2O + 2e^- \rightarrow Zn + 2OH^- \quad \text{(slow)} \tag{2'}$$

besides the fact that oxygen would have to diffuse through the pores to reach the cuprous oxide particles.

4. Conclusions

Copper and brass electrodes aged at OCP in aerated borax solution attain similar and stable values after 1 h of immersion. However, the film that develops after 24 h presents interesting differences, as regards composition and thickness. The film on brass seems to be dominated by the incorporation of Zn(II) compounds. Moreover, the film tends to be thicker but the presence of pores and defects produce a layer which is much less resistant than the one on copper.

Oxygen reduction on both materials is inhibited by the oxidation process, and the inhibition degree is higher for brass. The reduction

seems to proceed through a CE mechanism, similar to that observed for pre-reduced copper, where the oxides play a key role.

In the case of copper, the presence of a surface layer does not influence the limit current density, the global number of electrons exchanged or the Tafel slopes. Four electrons are exchanged, while the Tafel slope is ca. −0.3 V per decade, in agreement with the presence of a CE mechanism.

On brass, the oxygen reduction curves are dominated by a current peak associated to the reduction of the surface compounds and no clear limiting current can be observed until the surface film has been completely reduced. Assuming that the current registered at potentials negative to the peak can be considered as a limiting current, the number of exchanged electrons is close to 4.

Acknowledgements

The authors acknowledge the financial support received from the National Research Council of Argentina, CONICET, as well as from the Universidad Nacional de Mar del Plata.

References

[1] K.G. Boto, L.F.G. Williams, J. Electroanal. Chem. 77 (1977) 1.
[2] F. King, M.J. Quinn, C.D. Litke, J. Electroanal. Chem. 385 (1994) 45.
[3] A.P. Yadav, A. Nishikata, T. Tsuru, J. Electroanal. Chem. 585 (2005) 142.
[4] A.E.S. Sleightholme, J.R. Varcoe, A.R. Kucernak, Electrochem. Commun. 10 (2008) 151.
[5] M.V. Vázquez, S.R. de Sánchez, E.J. Calvo, J. Electroanal. Chem. 374 (1994) 179.
[6] S.M. Ceré, M.V. Vazquez, S.R. de Sánchez, D.J. Schiffrin, J. Electroanal. Chem. 470 (1999) 31.
[7] I. Milosev, H.-H. Strehblow, J. Electrochem. Soc. 150 (2003) B517.
[8] R. Procaccini, S. Ceré, M. Vázquez, J. Appl. Electrochem. 39 (2009) 177.
[9] S.R. de Sánchez, L.E.A. Berlouis, D.J. Schiffrin, J. Electroanal. Chem. 307 (1991) 73.
[10] ZView for Windows, ver. 3.0, Scribner Associates Inc., 2007.
[11] J. Gallardo, A. Durán, J.J. de Damborenea, Corros. Sci. 46 (2004) 795.
[12] L.J. Alijnovic, S. Gudic, M. Smith, J. Appl. Electrochem. 30 (2000) 973.
[13] Z plot for Windows, Electrochemical Impedance Software Operating Manual. Part I, Scribner Associates, Inc., Southern Pines, NC, 1998.
[14] R.E. Hummel, Phys. Stat. Solidi (a) 76 (1983) 11.
[15] B.-S. Kim, T. Piao, S.N. Hoier, S.-M. Park, Corros. Sci. 37 (1995) 557.
[16] C. Liu, Q. Bi, A. Leyland, A. Matthews, Corros. Sci. 45 (2003) 1243.
[17] M. Metikos-Hukovic, E. Tkalcec, A. Kwokal, J. Piljac, Surf. Coat. Technol. 165 (2003) 40.
[18] L.M. Abrantes, L.M. Castillo, C. Norman, L.M. Peter, J. Electroanal. Chem. 163 (1984) 209.
[19] M.V. Vázquez, S.R. de Sánchez, E.J. Calvo, D.J. Schiffrin, J. Electroanal. Chem. 374 (1994) 189.
[20] A.J. Bard, L.R. Faulkner, Electrochemical Methods. Fundamentals and Applications, John Wiley & Sons, New York, 1980, p. 110.